



GENERALIZED CRACK-TIP ENRICHMENT FUNCTIONS FOR X-FEM SIMULATION IN PIEZOELECTRIC MEDIA

BHARGAVA R.R. AND KULDEEP SHARMA*

Department of Mathematics, Indian Institute of Technology, Roorkee-247667, Uttarakhand, India

*Corresponding Author: Email- kuldeppurc@gmail.com

Received: December 12, 2011; Accepted: January 15, 2012

Abstract- The standard six crack-tip enrichment functions defined for piezoelectric media show an anomaly associated to their modified radii. It is found that these standard enrichment functions are not working for all the piezoelectric materials. To remove this anomaly, a generalized set of crack-tip enrichment functions are proposed here by redefining the existing basis functions. This would work for all the piezoelectric materials. The efficiency of these proposed enrichment functions are validated to Griffith's crack in an infinite domain with the energy norm and Intensity factors (IFs) convergence. The results obtained using X-FEM is also compared with the finite element method or without enrichment case on the same structured mesh.

Keywords- Crack-tip, Enrichment functions, Griffith's crack, Lekhnitskii's formalism, Level set, Piezoelectric

Citation: Bhargava RR and Kuldeep Sharma (2012) Generalized Crack-Tip Enrichment Functions for X-Fem Simulation in Piezoelectric Media. Journal of Information and Operations Management ISSN: 0976-7754 & E-ISSN: 0976-7762, Volume 3, Issue 1, 2012, pp-166-169.

Copyright: Copyright©2012 Bhargava R.R. and Kuldeep Sharma. This is an open-access article distributed under the terms of the Creative Commons Attribution License, which permits unrestricted use, distribution, and reproduction in any medium, provided the original author and source are credited.

Introduction

Piezoelectric ceramics are extensively used in high-tech apparatus as a key component of sensors/actuators/transducers. Due to the fatigue and aging cracks develop in them. Consequently it is imperative to investigate the fracture behaviour of such materials.

The extended finite element method (X-FEM) proposed by

Möes et al. [1], Black et al. [2] has proven to be a very efficient tool for the numerical modeling of cracks in LEFM. Recently, Béchet and his co-workers [3] have successfully applied the X-FEM to investigate enrichment schemes and their convergence for semi-infinite crack and Griffith-Irwin crack weakening a piezoelectric material having arbitrary polarization direction. They developed a set of six basis functions for the crack modeling in piezoelectric materials using analytic calculation based on Lekhnitskii's formalism and William's Eigen function approach. Bhargava and Sharma [4] applied the X-FEM with the four basis functions to study the finite specimen effects in 2-D piezoelectric media.

The objective of this work is to highlight the anomaly associated to modified radii of the six standard crack-tip enrichment functions with respect to different existing piezoelectric materials. Further, a

more generalized set of six crack-tip enrichment functions is proposed here for 2-D piezoelectric media in the framework of the X-FEM. The polarization is taken in an arbitrary direction to the crack axis and imposing impermeable conditions on the crack surface. The IFs are obtained using interaction integral in conjugation with the Stroh formalism.

Extended finite element approximation

Modeling of cracks using FEM is cumbersome in 2-D for complex structures or crack geometries. But X-FEM models crack(s) geometry independent of the mesh leading to a simplification in mesh generation and avoids remeshing as the crack grows.

The X-FEM exploits the partition of unity property of FEM first identified by

Möes et al. [1], which allows local enrichment functions to be easily incorporated into a finite element approximation. A standard approximation is thus enriched in a region of interest by the local functions in conjunction with additional degrees of freedom. For crack problems the enrichment functions are the near tip asymptotic fields and a discontinuous function to represent the jump in the displacement across the crack boundary.

To represent a crack, Level Set Method (LSM) has been applied which is proposed by Osher and Sethian [5]. One normal level set

function, ψ_1 , that is the signed distance to the union of the crack and the tangent extension from its front, and another tangent level

set function, ψ_2 , that is the signed distance function to a surface that passes by the crack boundary and is normal to the crack. The

crack surface is defined as the subset of the zero level set of ψ_1

where ψ_2 is negative. The crack front is defined as the intersection of the two zero level sets.

The extended finite element approximation for the displacement and electric potential can be written as follows

$$\begin{aligned}
 u^h(x,y) &= \sum_{I \in N} N_I(x,y) u_I + \sum_{I \in N^{cr}} N_I(x,y) (H(f^h(x,y)) - H(f_I)) a_I \\
 &+ \sum_{I \in N^{TIP}} N_I(x,y) \sum_{k=1}^6 (F^k(r, \theta, a_k^{re}, a_k^{im}) - F^k(x_I, y_I, a_k^{re}, a_k^{im})) b_I^k \\
 \phi^h(x,y) &= \sum_{I \in N} N_I(x,y) \phi_I + \sum_{I \in N^{cr}} N_I(x,y) (H(f^h(x,y)) - H(f_I)) c_I \\
 &+ \sum_{I \in N^{TIP}} N_I(x,y) \sum_{k=1}^6 (F^k(r, \theta, a_k^{re}, a_k^{im}) - F^k(x_I, y_I, a_k^{re}, a_k^{im})) d_I^k
 \end{aligned} \tag{2}$$

where $H(f(x,y))$ is a modified Heaviside step function

$$H(z_1) = \begin{cases} -1 & \text{if } z_1 < 0 \\ +1 & \text{if } z_1 > 0 \end{cases} \tag{3}$$

and the shape functions, $N_I(x,y)$, are isoparametric linear quadrilateral element shape functions that construct the partition of

unity. The column matrices u_I and ϕ_I are the nodal displacements and electric potential respectively, and a_I , b_I^k and c_I ,

d_I^k are the additional parameters.

where

$$r = \sqrt{(x - x_{tip})^2 + (y - y_{tip})^2}, \quad \theta = a \tan 2(y, x)$$

is the four-quadrant inverse tangent function;

N = the set of all nodes in the discretization;

N^{TIP} = the set of all nodes that are connected to elements containing crack tip(s);

N^{cr} = the set of nodes that are connected to elements containing the crack but not in N^{TIP} .

The set of nodes elected for enrichment are shown in Fig.

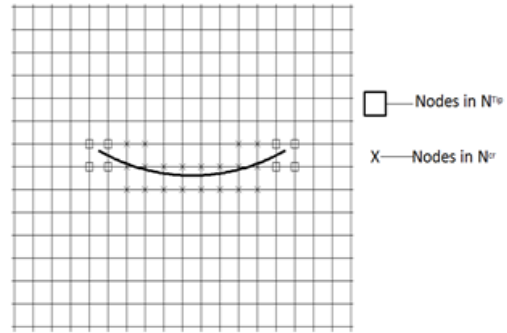


Fig. 1- The set of nodes elected for enrichment

Substituting the approximate displacement from Eq. (2) and the electric potential from Eq. (3) into the weak form illustrated in Piefort and Preumont [6], the standard discrete system of equations is obtained

$$K^s d = f^{ext} \tag{4}$$

where f^{ext} is the vector of external nodal forces and K^s the stiffness matrix.

The standard six crack-tip enrichment functions [3] are defined as

$$g(r, \omega) = \{ \sqrt{r} f_1(\omega), \sqrt{r} f_2(\omega), \sqrt{r} f_3(\omega), \sqrt{r} f_4(\omega), \sqrt{r} f_5(\omega), \sqrt{r} f_6(\omega) \} \tag{5}$$

where

$$f_m(\omega) = \begin{cases} \rho_m(\omega, a_m^{re}, a_m^{im}) \cos\left(\frac{\psi_m(\omega, a_m^{re}, a_m^{im})}{2}\right) & \text{if } a_m^{im} > 0, \\ \rho_m(\omega, a_m^{re}, a_m^{im}) \sin\left(\frac{\psi_m(\omega, a_m^{re}, a_m^{im})}{2}\right) & \text{if } a_m^{im} \leq 0. \end{cases} \tag{6}$$

The complex numbers $a_m = a_m^{re} + i a_m^{im}$ are the six roots of the characteristic equation A.5 defined in the Appendix. The modified angle and radius have the form

$$\psi_m(\omega, a_m^{re}, a_m^{im}) = \frac{\pi}{2} + \pi \operatorname{int}\left(\frac{\omega}{\pi}\right) - \arctan\left(\frac{\cos\left(\omega - \pi \operatorname{int}\left(\frac{\omega}{\pi}\right)\right) + a_m^{re} \sin\left(\omega - \pi \operatorname{int}\left(\frac{\omega}{\pi}\right)\right)}{|a_m^{im}| \sin\left(\omega - \pi \operatorname{int}\left(\frac{\omega}{\pi}\right)\right)}\right), \tag{7}$$

$$\rho_m(\omega, a_m^{re}, a_m^{im}) = \frac{1}{\sqrt{2}} \sqrt{(a_m^{re})^2 + (a_m^{im})^2 + (a_m^{re}) \sin 2\omega - [(a_m^{re})^2 + (a_m^{im})^2 - 1] \cos 2\omega}, \tag{8}$$

$$\omega = \theta - \phi.$$

where

Eqs. (7) and (8) assure that there are only three distinct values of modified angle and radius corresponding to eigenvalues with positive imaginary part, the rest are same to their respective conjugate parts.

Material dependence/independence of standard enrichment functions defined for piezoelectric material

If the roots of the characteristic Eq. (A.5) are purely an imaginary then

$$\rho_m(\omega, a_m^{re}, a_m^{im}) = \frac{1}{\sqrt{2}} \sqrt[4]{(a_m^{im})^2 + [1 - (a_m^{im})^2] \cos 2\omega} \tag{9}$$

Now, if $(a_m^{im})^2 < 0.5$ then sign of $(a_m^{im})^2 + [1 - (a_m^{im})^2] \cos 2\omega$ depends on $\cos 2\omega$.

Further, we know that ω lies between $-\pi$ to π , therefore the

possibility of $(a_m^{im})^2 + [1 - (a_m^{im})^2] \cos 2\omega$ to be negative

cannot be neglected. Hence, ρ_m is imaginary. There may be several cases possible where the position of the crack tip(s) and the Gauss point(s) of the blending element(s) or the crack tip ele-

ment(s) are in such a way that ρ_m is imaginary. Fig. 2 shows one of the same cases at the marked Gauss points for PZT-6B.

Table 1 presents the roots of the characteristic Eq. (A.5) with positive imaginary part for different piezoelectric materials. The poling direction is taken as perpendicular to the crack axis. The material constants for PZT-6B, PZT-PIC 151 and P-7 are taken from [7].

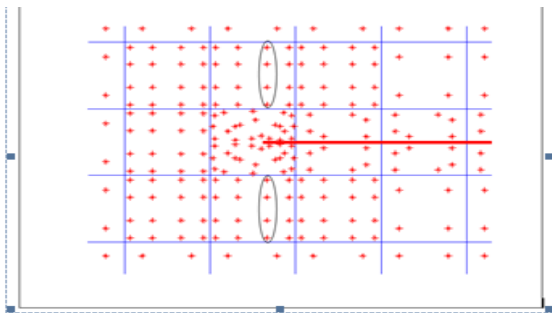


Fig. 2- Anomaly associated with the standard basis functions at the marked Gauss points

Table-1 - Eigen values with positive imaginary part of different piezoelectric materials at polarization angle, $\phi = 0$

Piezoelectric Material Constants	Eigen values with positive imaginary part
PZT-6B	0.5176i, 1.0143i, 2.1015i
PZT-PIC151	0.1904i, 1.1351i, 2.2718i
P-7	0.1795i, 0.9561i, 2.1951i

It is observed from Table 1 that one of the eigenvalues is purely

imaginary with $(a_m^{im})^2 < 0.5$. This implies that for all the above mentioned materials, there is always a possibility of finding a Gauss point at blending element(s) or crack tip element(s) where modified radius is imaginary. Therefore, the standard six enrichment functions for crack tip could not be guaranteed to precisely

represent the crack tip solution or to represent the field variables near the crack tip, which are actually real in nature.

Generalized set of crack-tip enrichment functions

In above section, we noticed that there is a need to redefine the modified radii of the standard enrichment functions otherwise it would not be applicable to all the piezoelectric materials. Here, we redefine the modified radius

$$\rho_m^*(\omega, a_m^{re}, a_m^{im}) = \frac{1}{\sqrt{2}} \sqrt[4]{(a_m^{re})^2 + (a_m^{im})^2 + (a_m^{re}) \sin 2\omega - [(a_m^{re})^2 + (a_m^{im})^2 - 1] \cos 2\omega} \tag{10}$$

$$T_m(\omega) = \begin{cases} \rho_m^*(\omega, a_m^{re}, a_m^{im}) \cos\left(\frac{\psi_m(\omega, a_m^{re}, a_m^{im})}{2}\right) & \text{if } a_m^{im} > 0, \\ \rho_m^*(\omega, a_m^{re}, a_m^{im}) \sin\left(\frac{\psi_m(\omega, a_m^{re}, a_m^{im})}{2}\right) & \text{if } a_m^{im} \leq 0. \end{cases} \tag{11}$$

where

in such a way so that ρ_m^* is always a real and positive value. Hence, the new generalized set of crack-tip enrichment functions are defined as

Our next objective is to show that the results obtained using generalized set of crack-tip enrichment functions are accurate in nature. This has been established by obtaining the energy and IFs convergences of the X-FEM results for Griffith-Irwin crack in an infinite domain. The results are also compared with finite element method or without enrichment case on the same structured mesh. The material used for this analysis is PZT-6B with polarization angle set

to be equal to $\pi/3$. The geometry, crack length and the applied loading are considered as shown in Fig.3.

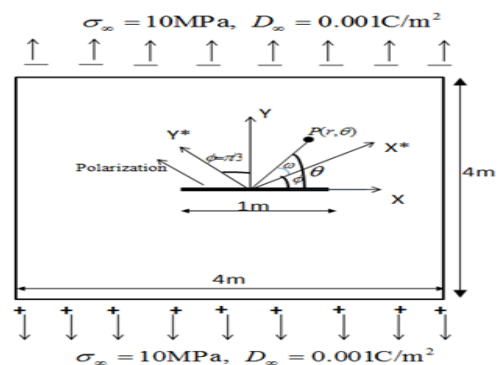


Fig. 3- Model geometry of the Griffith's crack for finite computation

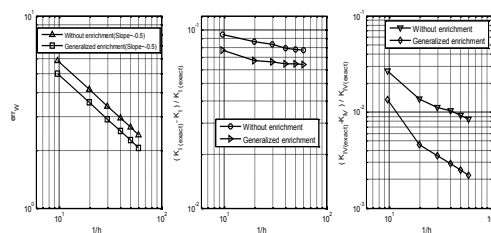


Fig. 4- Convergence study for PZT-6B under generalized set of crack-tip enrichment functions

Fig. 4 presents the energy and IFs convergences versus $1/h_e$ for the generalized set of enrichment functions and without enrichment case.

It clearly shows the energy norm and IFs convergence for X-FEM results obtained using generalized set of crack tip enrichment functions with respect to Griffith crack domain.

Further, an optimal rate -0.5 is also obtained for the energy norm convergence in conjugation to topological enrichment case. It is also noted that the obtained X-FEM results are far better than the ones achieved by using without enrichment case. Hence, the proposed enrichment functions defined here are considered to be the generalized crack-tip enrichment functions for the piezoelectric materials.

Conclusions

It is found that the six standard enrichment functions are not applicable to all the piezoelectric materials by means of the X-FEM. Therefore, generalized set of the crack-tip enrichment functions are proposed here, which are applicable to all the piezoelectric materials having a generalized case of crack and poling position.

Appendix

Assuming the plain strain conditions, the constitutive equations can be written as

$$\begin{Bmatrix} \epsilon_{xx} \\ \epsilon_{yy} \\ 2\epsilon_{xy} \end{Bmatrix} = \begin{bmatrix} a_{11} & a_{12} & a_{13} \\ a_{21} & a_{22} & a_{23} \\ a_{31} & a_{32} & a_{33} \end{bmatrix} \begin{Bmatrix} \sigma_{xx} \\ \sigma_{yy} \\ \sigma_{xy} \end{Bmatrix} + \begin{bmatrix} b_{11} & b_{21} \\ b_{12} & b_{22} \\ b_{13} & b_{23} \end{bmatrix} \begin{Bmatrix} D_x \\ D_y \end{Bmatrix} \tag{A.1}$$

$$\begin{Bmatrix} E_x \\ E_y \end{Bmatrix} = - \begin{bmatrix} b_{11} & b_{12} & b_{13} \\ b_{21} & b_{22} & b_{23} \end{bmatrix} \begin{Bmatrix} \sigma_{xx} \\ \sigma_{yy} \\ \sigma_{xy} \end{Bmatrix} + \begin{bmatrix} d_{11} & d_{12} \\ d_{12} & d_{22} \end{bmatrix} \begin{Bmatrix} D_x \\ D_y \end{Bmatrix} \tag{A.2}$$

where coefficients a_{ij} , b_{ij} and d_{ij} are reduced elastic, piezoelectric and dielectric constants, respectively defined in [3].

Now using extended Lekhnitskii's formalism to piezoelectric solids, the following potential function representation is introduced

$$\sigma_{xx} = \frac{\partial^2 F}{\partial y^2}; \sigma_{yy} = \frac{\partial^2 F}{\partial x^2}; \sigma_{xy} = -\frac{\partial^2 F}{\partial x \partial y};$$

$$D_x = \frac{\partial \psi}{\partial y}; D_y = -\frac{\partial \psi}{\partial x}$$

$F(x, y)$ and $\psi(x, y)$

where are complex potential functions.

It can be shown that the equilibrium equations are automatically satisfied by equation (A.3). Using the strain and electric field compatibility equations, the following sixth order differential equation

can be derived for $F(x, y)$

$$D_1 D_2 D_3 D_4 D_5 D_6 F = 0 \tag{A.4}$$

$$D_n = \left(\frac{\partial}{\partial y} - a_n \frac{\partial}{\partial x} \right), \text{ and } a_n (n = 1, \dots, 6)$$

where are the roots of the characteristic equation

$$P(a_i) = l_1(a_i)l_3(a_i) + l_2^2(a_i) = 0 \tag{A.5}$$

and

$$l_1(a_i) = d_{11}a_i^2 - 2d_{12}a_i + d_{22};$$

$$l_2(a_i) = b_{11}a_i^3 - (b_{21} + b_{13})a_i^2 + (b_{12} + b_{23})a_i - b_{22};$$

$$l_3(a_i) = a_{11}a_i^4 - 2a_{13}a_i^3 + (2a_{12} + a_{33})a_i^2 - 2a_{23}a_i + a_{22}. \tag{A.6}$$

References

- [1] Moes N., Dolbow J. and Belytschko T. (1999) *International Journal for Numerical Methods in Engineering*, 46,131-150.
- [2] Belytschko B.T., Black T. (1999) *International Journal for Numerical Methods in Engineering*, 45, 601-620.
- [3] Béchet E., Scherzer M. and Kuna M. (2009) *International Journal for Numerical Methods in Engineering*, 77, 1535-1565.
- [4] Bhargava R.R., Sharma K. (2011) *Computational Materials Science*, 50, 1834-1845.
- [5] Osher S., Sethian J.A. (1988) *Journal of Computational Physics*, 79, 12-49.
- [6] Piefort V., Preumont A. (2001) *Active Structures Laboratory, ULB-CP*, 165/42.
- [7] Li Q., Chen Y.H. (2007) *Journal of Applied Mechanics*, 74, 833-844.